IIETA International Information and Engineering Technology Association
Advancing the World of Information and Engineering

Mathematical Modelling of Engineering Problems
Vol. 8, No. 3, June, 2021, pp. 461-466
Journal homepage: http://iieta.org/journals/mmep

Distortion Control for Dissimilar Welding of SS321 to Hastelloy C-276 with CO_2 Laser Beam Butt Joints Using Taguchi Methods

Gandu Guruvaiah Naidu*, Sarojini Jajimoggala

GIT, GITAM, Visakhapatnam 530045, Andhra Pradesh, India

Corresponding Author Email: guruvaiahnaidu.g@gmail.com

https://doi.org/10.18280/mmep.080317

Received: 12 September 2020
Accepted: 20 April 2021

Keywords:
laser beam welding, dissimilar materials, orthogonal array, distortion, ANOVA

ABSTRACT

The laser beam welding process is a promising technology because of its reliability and ability to automate the process easily. This study aims to analyze distortion for dissimilar laser weld joints. Hastelloy C276 and SS321 plates are joined by using the CO_2 Laser beam welding. Welding current, welding speed and shielding gas flow are chosen as process parameters for preparing butt joints. Each of the factors has two levels to control the parameters of the output. Experimentation was conducted with four trails by using an L4 orthogonal array. The quality of the welds and bead geometry are verified through macrostructure examination. The Vernier height gauge was used for the measurement of distortion in the weldments. Lower the better-quality characteristic is chosen for the response. ANOVA studies identified laser power at 81%, the weld speed at 16% parameters is a contribution with a statistical of about 95%. Full penetration was observed for all the experimental trails.

1. INTRODUCTION

Hastelloy C-276 has been widely used in turbine structures, chemical plants, gas and oil industries, nuclear applications etc., due to its high thermal and corrosion resistance properties. Arc welding is widely used in the joining of similar and dissimilar materials using multipass welding. In multipass welding, the high heat input will affect the lattice spacing and affect the weld's mechanical and microstructural and results low joint efficiency. The use of lasers for joining and cutting metals is rising in industrial applications and other engineering components because of its concentrated high-power density at a localized area, resulting in a very narrow heat-affected zone [1, 2]. By using the laser beam welding process, increased productivity can be achieved with improved structural and mechanical properties. Ni-based alloys' joining was rising with an increase in demand for stiff structures used at high-temperature applications. The quality of the weld joints can be made using the high beam welding process. The effect of heat input in the welds is reported for mechanical and microstructural properties [3-5].

Harinadh et al. [6-8] had reported the importance of distortion formed during the arc and beam welding process for similar and dissimilar joints. Vernier height gauges used for measuring the distortion in the weldments. L_4 and L_9 orthogonal arrays used for experimentation. The critical parameter which influences the distortion were identified by using the ANOVA techniques, distortion in the weldment is varied due to the coefficient of thermal expansion and the base materials' thermal conductivity. Welding current, welding speed is showing more criticality for distortion for the beam welding process. Root gap and welding current are identified as influencing parameters in gas tungsten arc welding. Zhou et al. [9, 10] conducted dissimilar experiments for C-276 to SS304 materials. The laser beam welding process was used for the experimentation to produce overlap-joints. The authors had reported microstructure and mechanical properties, and the inter-dendrite precipitated phases were observed; which might be possibly due to p or μ phases. Tensile failure was at the weld zone, and the strength was reduced by 17% of C-276 material.

Many authors reported dissimilar welding [11-13] of Hastelloy C276 and with stainless steel materials using the GTAW process. to study the microstructural and mechanical behaviour. Due to the increase in heat input in the GTAW process, the conspicuous coarse grains are formed in both the base materials. Devendranath et al. [14] used the pulsed current GTAW process for joining Hastelloy C-276 and investigated the welds' micro and mechanical properties. The structural integrity of the weld was improved by using the laser peening process of the GTAW weldment. The comparison of the yield strength is considered before and after laser peening. The improved mechanical strength of the laser beam weldments of Hastelloy C-276 has observed by using the post-weld heat treatment with different heating and cooling cycles [15-17]. The authors extensively studied microstructure and mechanical properties concerning heat input based on the reported literature, further, to improve the strength of the weldments using post welded heat treatment. Before the actual welding process's commencement, the post-weld distortion can be controlled using the clamping method during the welding process [18, 19]. Post distortion can be controlled by the laser shock processing method [20].

Joining dissimilar materials is always challenging because of the different thermal and mechanical properties of the base materials. The measurements of distortion for various manufacturing processes reports have been made in several works of literature. Unfortunately, the distortion by considering the effects such as laser power, welding speed, for dissimilar welding, and single-pass (square butt joint) welding

is underexplored and needed much attention. This work employs the square butt joint for dissimilar welding of Hastelloy C-276 to SS321 of 5mm thick plates using the CO_2 laser beam welding process. Further, L4 orthogonal array is used with two levels and the three factors for optimizing. This study will help us to understand the effect of each parameter and their levels influencing the distortion. The angular distortion in the final welds was measured with a vernier height gauge. The No-way analysis is used to estimate these parameters critical or not and Analysis of Variance (ANOVA) analysis has been used to detect angular distortion essential factors of the final dissimilar welds.

2. EXPERIMENTAL PROCEDURE

The base materials used for this study were SS321, and Hastelloy C-276. The chemical composition of the parent materials is provided in Table 1. The base materials dimensions are 110 mm x 80 mm x 5mm thick plates. Prior to actual experimentation, the sample was machined using the wire cut electric discharge machining (EDM) at the butt surface to avoid sharp edges and foreign particles. CO_2 Laser beam welding [2, 21, 22] processes for the current experimentation is displayed in Figure 1. The controllable factors employed for joining dissimilar materials of SS321 and Hastelloy C-276 are given in Table 2, which refers to experimental input as per the L_4 orthogonal array [23] with the matrix; each parameter (Laser power, welding speed and shielding gas) taken at two levels. Before starting the actual experimentation, the bead on plate trails was carried out to identify the best combinations for joints. Table 3 gives the fixed technical specifications which were used in the experimentation. The experimentation matrix was carried out using the parameters shown in Table 6 and the final welds, as displayed in Figure 2. The weldments have undergone a quality check with a visual inspection for surface cracks and internal defects using X-Ray radiography techniques. All the weldments are free from defects.

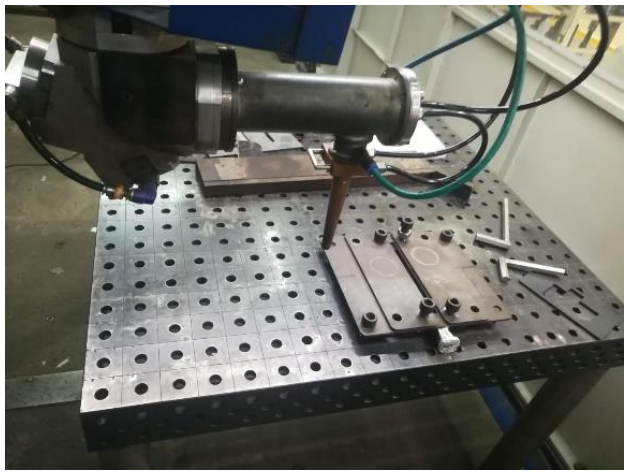

(a)

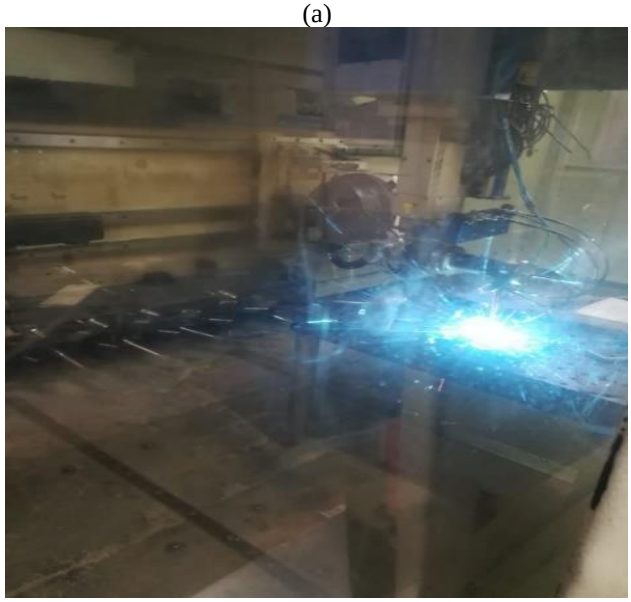

(b)

Figure 1. Photographs demonstrating experimental set-up for laser beam welding

Table 1. Base materials chemical composition (% by mass)

	Ni	Cr	Mo	W	Fe	Mn	V	Others
C-276	58.47	15	15.6	3.36	6.24	0.38	0.58	P 0.03, S 0.01, Co 0.71, C 0.01, Si 0.04
SS321	9.18	17.3	0.27	-	71	0.94	0.23	Nb 0.02, Cu 0.35

Table 2. Controllable factors with levels

S.No	Parameters	Units	$Level_1$	$Level_2$
1	Laser beam power	kW	3.0	3.5
2	Welding speed	m/min	1.0	1.5
3	Flow rate	LPM	10	15

Table 3. Technical specifications of the laser system

S.No	Parameters	Values
1	Maximum output laser power (kW)	4.0
2	Frequency (Hz)	20000
3	Focal length (mm)	39
4	Focal spot diameter (mm)	2
5	Beam position	At surface

Figure 2. Picture of the welded samples of dissimilar joints

2.1 Calculation of heat input

The microstructure and mechanical properties of the weldments are varied due to weld heat input. Heat input will differ with based on controllable process parameters. The calculation of heat input [2] for each experimental trial is carried out using Eq. (1).

$$HI = \frac{0.6W}{V} \quad (1)$$

whereas W is the welding current, V is welding speed Q - heat input (based on thermal efficiency) was set as 0.6.

2.2 Distortion

During the welding process, the material experiences heating and cooling cycles in the weld; and thus, undergoes dimensional changes in the weld structure which is called distortion. Distortion in the welds will be in the longitudinal and transverse direction, as shown in Figure 3. Measurement of angular distortion is carried out using vernier height [2, 24], and calculation was carried out by using the Eq. (2).

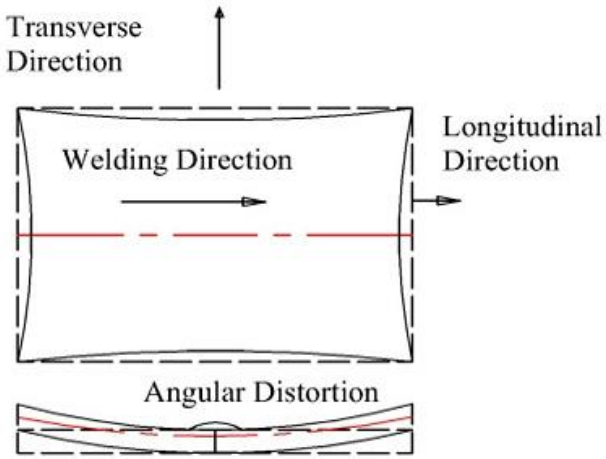

Figure 3. Types of distortion in the welds

$$\alpha = \sin^{-1}\left[\frac{h_1 - h_2}{b}\right] \quad (2)$$

where, h_1= total height at vernier height, h_2= total height of the workpiece from the surface and b=distance of the workpiece. For both the responses, lower the better-quality characteristics were chosen for the responses.

3. RESULTS AND DISCUSSION

3.1 Weld quality

The quality of the weldments is verified using the macrostructure examination. The solid solubility of both the base materials at the fusion zone is given by bead geometry. All four samples have undergone microstructure examination to empower the weld bead dimensions and access the weld quality. The measurement is taken at the top and middle portions of the weldment in the horizontal direction. Higher the better depth of penetration and lower the bead width is recommended for the weld joints. In all the trails, the full penetration was seen with a good mixture of base materials and forms a sound bead width as given in Figure 4.

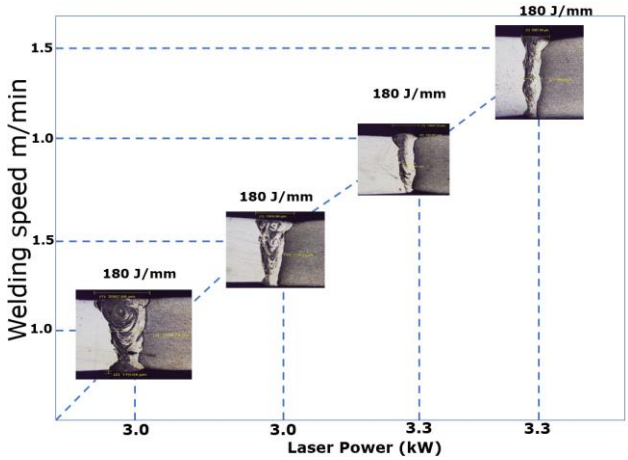

Figure 4. Weld bead geometry of the final laser welds

The quality characteristic of heat input and distortion are chosen as lower the better. The selected factors, as given Table 2, may be critical or may not be for the desired responses. The criticality of the responses can be accessed by using the No-Way ANOVA analysis. Calculation of heat input in trails is done by using the Eq. (1). Angular distortion in the weldment measured on the weld's top surface by using the vernier gauge is shown in Figure 5. Effect of Heat Input on the final welds are given in Table 4 with full experimental matrix and final responses. The lower heat input observed for trail-2 is 120 kJ/mm, maximum for trail-4 is 140 kJ/mm. The least distortion was 1.32° for trail-2 and the maximum was seen 1.55° for trail-1.

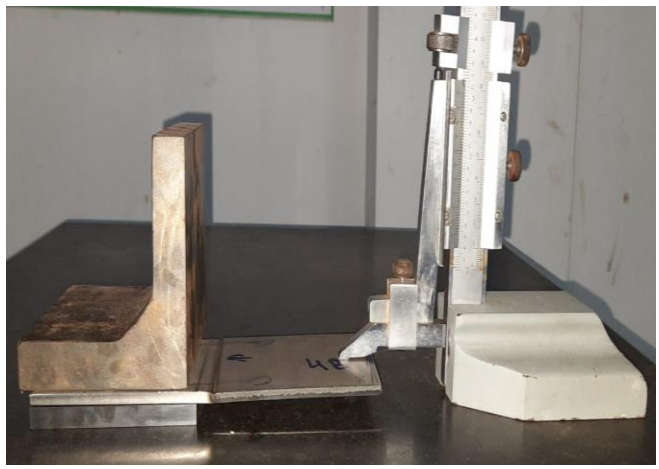

Figure 5. Measurement of distortion in the final welds using vernier height gauge

The intention of this analysis to find the optimized factors for the least distortion in the welds. Heat input and distortions for all the trails are given in Table 4. The distribution of distortion in the welds are in Figure 5. From the experimental responses from Table 4, it was seen that trail-2 shows the least distortion with laser power at 3.0 kW, welding speed at 1.5 m/min and shielding gas at 15 LPM. From all the trails all experimental trails show the full penetration. The graphs show a similar trend in the results.

3.2 No-way ANOVA analysis

In No-Way analysis, no factor is discussed in this assessment; only the deviation of the data is seen from its mean value, which is always a straight line as displayed in Figure 5; another line is the deviation of response about the mean value for all the trails. This analysis helps us to ensure the criticality of the selected parameters. For the 4 experiments, the variation of distortion variation to mean average is given in Figure 6. The calculated values of the sum of squares of the mean (SS_m) is 12.67, the total sum of squares (SS_T) is 13.25 and sum of squares of error (SS_e) is 0.57.

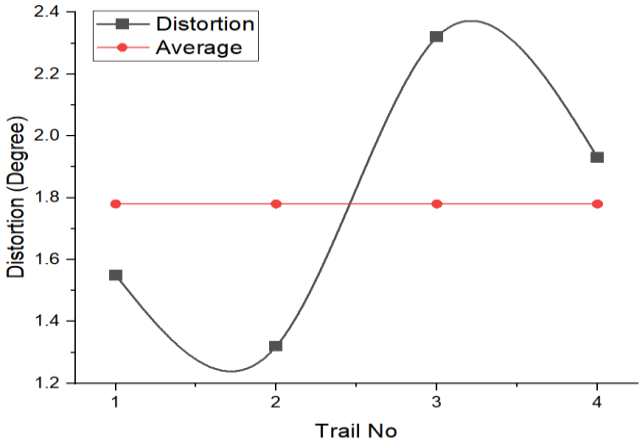

Figure 6. Distribution of distortion about average

The criticality between the process parameters assessed by using the No-Way ANOVA. From the analysis, it was noticed with 99% criticality from the experimental results. No-Way ANOVA calculated results is provided in Table 5. The null hypothesis rejected when $F_{0.01,v1,v2}$ is larger than $F_{calculated}$ value; in this case, the alternate hypothesis is accepted. For the current analysis, the $F_{calculated}$ value is greater than the $F_{tabulated}$ value than i.e., $F_{0.05,1,3}$ and $F_{0.01,1,3}$. The variance is showing 99% confidence. Hence, from the No-way ANOVA analysis, the chosen factors are critical for the response. Further, ANOVA is carried out to evaluate the confidence and % of each factor's contribution towards the response.

3.3 ANOVA analysis

Further, ANOVA analysis conducted to detect the critical factors and % of the criticality's contribution for a response. ANOVA analysis is carried out for the response, and the summary of ANOVA results are provided in Table 6. As $F_{caluculated}$ is superior to $F_{0.01,1,5}$, laser power selection is a critical factor. And it shows 95% confidence for distortion; hence, laser power needs to keep under control. Level 1 is 3.0 kW, and the distortion is 2.6° lower than level 2 of laser power 3.5 kW the distortion is 4.02°, with 81% of contribution as shown in Figure 7(a). The welding speed also shows 95% confidence to influence and 16.4% of the contribution for distortion. The welding speed at level-2 is 2.7°, and the level-1 level shows a higher distortion 3.86°; the contribution of welding speed and distortion are given in Figure 7(b). Shielding gas flow rate at level-1 gives lower distortion then level-2. But from ANOVA, Table 6 and Figure 7(c), the factor-C is not significant. But for producing defect-free joints shielding gas a critical role. Shielding gas protects the weld area from oxygen and water vapour. Depending on the materials being welded, these atmospheric gases can reduce the weld's quality or make the welding more difficult. The wrong choice of a welding gas can lead to a porous and weak weld or excessive spatter; the latter, while not affecting the weld itself, causes loss of productivity due to the labor needed to remove the scattered drops [8, 21, 22].

Table 4. Experimental plan with responses

Trail No/ Units	Parameters			Responses		
	Welding power	Welding Speed	Shielding gas flow rate	Heat input	Angular distortion	Penetration
	kW	mm/min	LPM	kJ/mm	θ	
1	3.0	1.0	10	180	1.55	Full
2	3.0	1.5	15	120	1.32	Full
3	3.5	1.0	15	210	2.32	Full
4	3.5	1.5	10	140	1.93	Full

Table 5. No-Way ANOVA for the experimental results

Source	SS	doF	Variance	$F_{calulated}$	$F_{0.1,1,3}$	$F_{0.05,1,3}$	$F_{0.01,1,3}$
Mean	12.67	1	12.67	65.71	5.54	10.1	34.1
Error	0.57	3	0.192				
Total	13.25	4					

Table 6. ANOVA summary for distortion results

Source	SS	doF,v	Variance, V	Ftable	$F_{0.1,1,5}$	$F_{0.05,1,5}$	$F_{0.01,1,5}$	Confidence	P, % Contribution
Welding power	0.47	1	0.4761	74.39	4.06	6.61	16.8	++	81.38
Welding speed	0.09	1	0.0961	15.01				++	16.42
Shielding gas flow	0.0064	1	0.0064	1					1.094
Error	0.0064	1	0.0064						1.094
SS_T	0.585	4							100

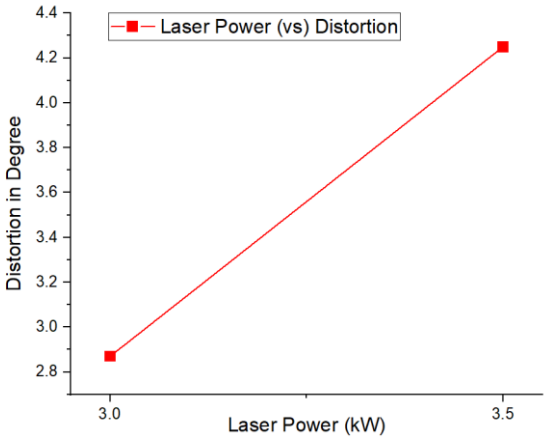

(a) Laser power effect on response

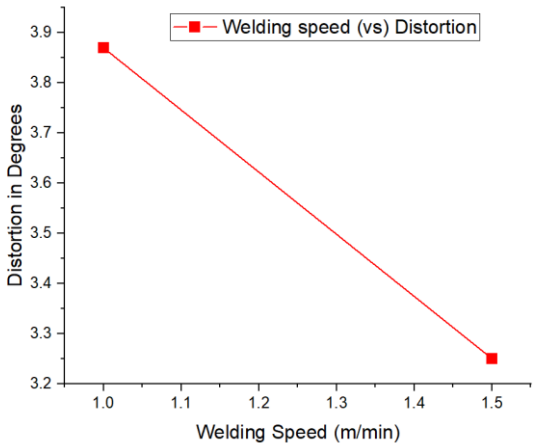

(b) Welding speed effect on response

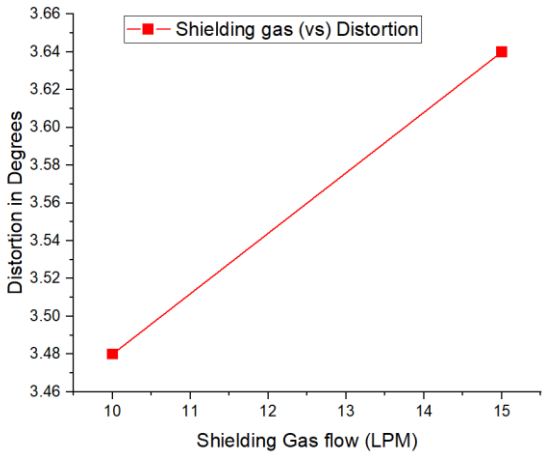

(c) Shielding gas flow effect on response

Figure 7. Contribution of process parameters for distortion

4. CONCLUSIONS

The CO_2 laser beam welding process is used to weld dissimilar materials with process parameters as laser power, welding speed and shielding with two levels for L4 orthogonal array. Radiography analysis is carried out for the final welds, and weldments were free from defects and porosity.

- Full penetration observed in all the trails with good weld bead geometry.
- The No-Way ANOVA confirmed that the experimental results are critical, with 99% confidence.
- From ANOVA analysis welding power and welding, speed are critical process parameters at 95% confidence.
- For least distortion in the laser beam weldment parameters recommended are laser power at level-1, 3.0kW and welding speed at level-2, 1.5mm/min.
- This procedure can be well utilized for dissimilar materials of SS321 to Hastelloy C-276 for the least distortion in the structures using the laser beam welding process.

REFERENCES

[1] Ma, G., Wu, D., Guo, D. (2011). Segregation characteristics of pulsed laser butt welding of Hastelloy C-276. Metallurgical and Materials Transactions A, 42(13): 3853-3857. https://doi.org/10.1007/s11661-011-0978-3

[2] Shanthos Kumar, G., Raghukandan, K., Saravanan, S., Sivagurumanikandan, N. (2019). Optimization of parameters to attain higher tensile strength in pulsed Nd: YAG laser welded Hastelloy C-276–Monel 400 sheets. Infrared Physics & Technology, 100: 1-10. https://doi.org/10.1016/j.infrared.2019.05.002

[3] Bal, K.S., Dutta Majumdar, J., Roy Choudhury, A. (2018). Study on uni-axial tensile strength properties of Ytterbium fiber laser welded Hastelloy C-276 sheet. Optics & Laser Technology, 108: 392-403. https://doi.org/10.1016/j.optlastec.2018.07.018

[4] Bal, K.S., Dutta Majumdar, J., Roy Choudhury, A. (2019). Investigation into the intergranular corrosion behaviour of electron beam welded Hastelloy C-276 sheet using laser displacement sensor. Measurement, 144: 345-365. https://doi.org/10.1016/j.measurement.2019.05.016

[5] Zain-ul-Abdein, M., Nelias, D., Jullien, J.F., Deloison, D. (2009). Prediction of laser beam welding-induced distortions and residual stresses by numerical simulation for aeronautic application. Journal of Materials Processing Technology, 209(6): 2907-2917. https://doi.org/10.1016/j.jmatprotec.2008.06.051

[6] Vemanaboina, H., Edison, G., Akella, S. (2018). Distortion control in multi pass dissimilar GTAW process using Taguchi ANOVA analysis. International Journal of Engineering & Technology, 7(3): 1140. https://doi.org/10.14419/ijet.v7i3.12607

[7] Vemanaboina, H., Naidu, G.G., Vinod Kumar, G., Ramachandra Reddy, D. (2019). Welding characteristics of butt-welded Inconel625 plate using CO_2 laser beam. Materials Today: Proceedings, 19(Part 2): 859-863. https://doi.org/10.1016/j.matpr.2019.08.223

[8] Vemanaboina, H., Akella, S., Ramesh Kumar, B. (2020). Distortion control in laser beam welding using Taguchi ANOVA analysis. FME Transactions, 48(1): 180-186. https://doi.org/10.5937/fmet2001180H

[9] Zhou, S., Chai, D., Yu, J., Ma, G., Wu, D. (2017). Microstructure characteristic and mechanical property of pulsed laser lap-welded nickel-based superalloy and stainless steel. Journal of Manufacturing Processes, 25: 220-226. https://doi.org/10.1016/j.jmapro.2016.11.010

[10] Zhou, S., Ma, G., Dongjiang, W., Chai, D., Lei, M. (2018). Ultrasonic vibration assisted laser welding of nickel-based alloy and Austenite stainless steel. Journal of Manufacturing Processes, 31: 759-767. https://doi.org/10.1016/j.jmapro.2017.12.023

[11] Pandit, S., Joshi, V., Agrawal, M., Manikandan, M., Ramkumar, K.D., Arivazhagan, N., Narayanan, S. (2014). Investigations on mechanical and metallurgical properties of dissimilar continuous GTA welds of monel 400 and C-276. Procedia Engineering, 75: 61-65. https://doi.org/10.1016/j.proeng.2013.11.012

[12] Manikandan, M., Arivazhagan, N., Nageswara Rao, M., Reddy, G.M. (2014). Microstructure and mechanical properties of alloy C-276 weldments fabricated by continuous and pulsed current gas tungsten arc welding techniques. Journal of Manufacturing Processes, 16(4): 563-572. https://doi.org/10.1016/j.jmapro.2014.08.002

[13] Sharma, S., Taiwade, R.V., Vashishtha, H., Mukherjee, S., Tiwari, S. (2018). Consumable selection for pulsed current gas tungsten arc welded bimetallic joints between Super C-276 alloy and Ti -stabilized Grade 321. Journal of Manufacturing Processes, 32: 32-47. https://doi.org/10.1016/j.jmapro.2018.01.018

[14] Devendranath Ramkumar, K., Narenthiran, A., Konjenti, A., Pravin, P.N., Kanish, T.C. (2019). Effect of low energy laser shock peening on the mechanical integrity of Hastelloy C-276 welds. Journal of Materials Processing Technology, 274: 116296. https://doi.org/10.1016/j.jmatprotec.2019.116296

[15] Wu, D., Ma, G., Guo, Y., Guo, D. (2010). Study of weld morphology on thin Hastelloy C-276 sheet of Study weld morphology on thin Hastelloy C-276 sheet of pulsed laser welding pulsed laser welding. Physics Procedia, 5: 99-105. https://doi.org/10.1016/j.phpro.2010.08.034

[16] Bal, K.S., Dutta Majumdar, J., Roy Choudhury, A. (2019). Effect of post-weld heat treatment on the tensile strength of laser beam welded Hastelloy C-276 sheets at different heat inputs. Journal of Manufacturing Processes, 37: 578-594. https://doi.org/10.1016/j.jmapro.2018.12.019

[17] Guo, Y., Wu, D., Ma, G., Guo, D. (2014). Trailing heat sink effects on residual stress and distortion of pulsed laser welded Hastelloy C-276 thin sheets. Journal of Materials Processing Technology, 214(12): 2891-2899. https://doi.org/10.1016/j.jmatprotec.2014.06.012

[18] Schenk, T., Richardson, I.M., Kraska, M., Ohnimus, S. (2009). Influence of clamping on distortion of welded S355 T-joints. Science and Technology of Welding and Joining, 14(4): 369-375. https://doi.org/10.1179/136217109x412418

[19] Li, J., Guan, Q., Shi, Y.W., Guo, D.L. (2004). Stress and distortion mitigation technique for welding titanium alloy thin sheet. Science and Technology of Welding and Joining, 9(5): 451-458. https://doi.org/10.1179/136217104225021643

[20] Tsai, C.L., Han, M.S. (2004). Thermal and mechanical evolution of welding-induced buckling distortion. Journal of the Chinese Institute of Engineers, 27(6): 907-920. https://doi.org/10.1080/02533839.2004.9670943

[21] Buddu, R.K., Chauhan, N., Raole, P.M., Natu, H. (2015). Studies on mechanical properties, microstructure and fracture morphology details of laser beam welded thick SS304L plates for fusion reactor applications. Fusion Engineering and Design, 95: 34-43. https://doi.org/10.1016/j.fusengdes.2015.04.001

[22] Arivarasu, M., Roshith, P., Padmanaban, R., Thirumalini, S., Phani Prabhakar, K.V., Padmanabham, G. (2017). Investigations on metallurgical and mechanical properties of CO_2 laser beam welded Alloy 825. Canadian Metallurgical Quarterly, 56(2): 232-244. https://doi.org/10.1080/00084433.2017.1315847

[23] Ross, P.J. (1986). Taguchi Techniques for Quality Engineering. 2nd ed. New York: McGraw-Hill.

[24] Parmar, R.S. (2010). Welding Engineering and Technology, Edition-2, Khanna Publishers.